

## Expression and Purification of Porcine Rotavirus Structural Proteins in Silkworm Larvae as a Vaccine Candidate

メタデータ	言語: eng 出版者: 公開日: 2022-08-17 キーワード (Ja): キーワード (En): 作成者: Kato, Tatsuya, Kakuta, Tatsuki, Yonezuka, Ami, Sekiguchi, Tomofumi, Machida, Yuki, Xu, Jian, Suzuki, Tohru, Park, Enoch Y. メールアドレス: 所属:
URL	<a href="http://hdl.handle.net/10297/00029087">http://hdl.handle.net/10297/00029087</a>

1 **Expression and purification of porcine rotavirus structural**  
2 **proteins in silkworm larvae as a vaccine candidate**

3 Tatsuya Kato<sup>1,2,3,\*</sup>, Tatsuki Kakuta<sup>2</sup>, Ami Yonezuka<sup>2</sup>, Tomofumi Sekiguchi<sup>3</sup>, Yuki  
4 Machida<sup>3</sup>, Jian Xu<sup>1,†</sup>, Tohru Suzuki<sup>4</sup>, Enoch Y. Park<sup>1,2,3</sup>

5  
6 <sup>a</sup> Molecular and Biological Function Research Core, Research Institute of Green  
7 Science and Technology, Shizuoka University, Ohya 836, Suruga-ku, Shizuoka, Japan.

8 <sup>b</sup> Department of Applied Life Science, Faculty of Agriculture, Shizuoka University,  
9 Ohya 836, Suruga-ku, Shizuoka, Japan.

10 <sup>c</sup> Department of Agriculture, Graduate School of Integrated Science and Technology,  
11 Shizuoka University, Ohya 836, Suruga-ku, Shizuoka, Japan.

12 <sup>d</sup> Division of Pathology and Pathophysiology, Hokkaido Research Station, National  
13 Institute of Animal Health, NARO, Sapporo, Hokkaido 062-0045, Japan.

14 <sup>†</sup> Present affiliation: Laboratory of Biology and Information Science, School of Life  
15 Sciences, East China Normal University, 3663 North Zhongshan Road, Shanghai,  
16 200062, PR China.

17  
18 \*Corresponding author.

19 Address: Molecular and Biological Function Research Core, Research Institute of Green  
20 Science and Technology, Shizuoka University, Ohya 836, Suruga-ku, Shizuoka, Japan.

21 Tel. & fax: +81-54-238-4937. E-mail address: kato.tatsuya@shizuoka.ac.jp (Tatsuya  
22 Kato)

23

24 **ABSTRACT**

25 In this study, silkworm larvae were used for expression of porcine rotavirus A (KS14  
26 strain) inner capsid protein, VP6, and outer capsid protein, VP7. Initially, VP6 was  
27 fused with Strep-tag II and FLAG tag (T-VP6), and T-VP6 was fused further with the  
28 signal peptide of *Bombyx mori* 30k6G protein (30k-T-VP6). T-VP6 and 30k-T-VP6 were  
29 then expressed in the fat body and hemolymph of silkworm larvae, respectively, with  
30 respective amounts of 330 µg and 50 µg per larva of purified protein. Unlike T-VP6,  
31 30k-T-VP6 was *N*-glycosylated due to attached signal peptide. Also, VP7 was fused  
32 with PA-tag (VP7-PA). Additionally, VP7 was fused with Strep-tag II, FLAG-tag, and  
33 the signal peptide of *Bombyx mori* 30k6G protein (30k-T-ΔVP7). Both VP7-PA and  
34 30k-T-ΔVP7 were expressed in the hemolymph of silkworm larvae, with respective  
35 amounts of 26 µg and 49 µg per larva of purified protein, respectively. The results from  
36 our study demonstrated that T-VP6 formed nanoparticles of greater diameter compared  
37 with the ones formed by 30k-T-VP6. Also, higher amount of VP6 expressed in silkworm  
38 larvae reveal that VP6 holds the potential for its use in vaccine development against  
39 porcine rotavirus with silkworm larvae as a promising host for the production of such  
40 multi-subunit vaccines.

41

42 **Keywords** Porcine rotavirus, VP6, VP7, Silkworm larvae, Vaccine

43

## 44 **Introduction**

45 Rotaviruses are non-enveloped viruses of the family Reoviridae that are major causes of  
46 acute gastroenteritis in infants and some species of animals [1]. Rotaviruses have 11  
47 segments of double-stranded RNA (ds-RNA) as their genome, encoding several  
48 structural (VP1, 2, 3, 4, 6, 7) and non-structural proteins (NSP1, 2, 3, 4, 5, 6). The viral  
49 genome is enclosed within a triple-layered capsid, which is composed of VP2, VP6, and  
50 VP7 proteins. Additionally, VP4, a viral hemagglutinin, has been found to form spikes  
51 that project from the outer layer of VP7, a viral capsid protein. Both VP4 and VP7 are  
52 known to facilitate binding of the mature viral particles to the cell surface receptors of  
53 the host cells [2, 3].

54 Recently, live attenuated oral vaccines (Rotarix, RotaTeq, etc.) have become  
55 available for human use. They are being extensively used globally, owing to their high  
56 efficiency in providing protection against rotavirus diseases. However, instances of their  
57 lower efficiency have occurred sporadically in some countries [4, 5] because children in  
58 low and middle-income countries suffer from reduced immune responses, malnutrition  
59 and maternal antibodies, and the oral administration of vaccines are easily influenced by  
60 gut microbial environment, gastric acidity and breast milk antibodies [6]. Moreover, the  
61 reassortment of live attenuated vaccines of the wild type is often challenging for safety  
62 reasons. Therefore, developing other effective rotavirus vaccines through different  
63 strategies, such as using viral subunits or virus-like particles (VLPs), can prove to be  
64 better alternatives to the currently available live attenuated vaccines. Recently, P2-VP8  
65 vaccine, which is composed of rotavirus VP8 fused with P2 CD4<sup>+</sup> epitope from tetanus  
66 toxin, has been developed in *Escherichia coli* expression system as an injectable  
67 vaccine and several clinical trials have also been done [7–9].

68 Previous studies have shown rotaviral capsid protein, VP6, as a potential candidate  
69 for the vaccine development [10]. VP6 is a major capsid protein that covers the inner  
70 capsid that is composed of VP2. The double-layered capsid particles are structurally  
71 formed when VP6 and VP2 are co-expressed in insect and plant cells [3, 11]. However, a  
72 single VP6 protein is produced in these hosts, while the *Escherichia coli* system produces  
73 VP6 nanoparticles or nanotubes [12–14]. Immunization of mice with tubular VP6, results  
74 in the production of VP6-specific IgG and IgA, as well as interferon- $\gamma$ -secreting CD4<sup>+</sup> T  
75 cells in their mucosal cells and serum [15]. The tubular form of VP6 was seen to possess  
76 an immunostimulatory effect, similar to that of an adjuvant, as observed in the RAW  
77 264.7 macrophage cell line [16].

78 According to some reports, immunization with VP6 expressed in plants as an oral  
79 vaccine, led to higher serum titers of VP6-specific IgG and saliva mucosal VP6-specific  
80 IgA [17]. Additionally, several plants (potato, corn seed, etc.) have been successfully  
81 used as hosts to express rotavirus structural proteins that can act as oral vaccines [18,  
82 19]. These results demonstrate that plants are promising hosts for the preparation of  
83 rotavirus subunit vaccines. Besides plants, silkworm (*Bombyx mori*) has also been  
84 shown as a promising host for producing a subunit vaccine using a baculovirus  
85 expression system [20, 21]. Silkworm larvae and pupae are known to produce  
86 recombinant proteins, and a large-scale production can be effortlessly carried out by  
87 increasing the number of silkworms. Yao et al. reported that VP2, VP6, and VP7 of  
88 rotavirus could be simultaneously expressed using a multi-gene baculovirus expression  
89 system, such as MultiBac in silkworm larvae (BmMultiBac). The expressed proteins  
90 when combined, could form round nanoparticles in the hemocytes of silkworm larvae  
91 [22].

92 This study focused on the production of VP6 and VP7 proteins from porcine  
93 rotavirus A (KS14 strain), which is associated with swine diarrhea. Our aim is the  
94 development of vaccines to porcine rotavirus A because no commercial vaccine to  
95 porcine rotavirus A are available. Now, some live attenuated oral vaccines (Rotarix,  
96 RotaTeq, etc.) are available for human, but non-live rotavirus vaccines, for example,  
97 subunit vaccines, are demanded [23]. To develop vaccines to porcine rotavirus A, we try  
98 to prepare purified VP6 and VP7 in silkworm larvae as subunit vaccines. An  
99 endogenous signal peptide in silkworm, 30 kDa lipoprotein (30k6G), present as a  
100 storage protein in its hemolymph, was attached to the two VP proteins to enhance  
101 protein purification from silkworm serum [24]. Subsequently, the expression patterns  
102 and the resulting particle formation of purified VP6 and VP7 proteins, with or without  
103 the signal peptide, were compared and investigated. The results from the current study  
104 show that a high amount of non-glycosylated VP6 protein is obtained from silkworm  
105 larvae. Moreover, well-formed VLPs were obtained in a silkworm-based baculovirus  
106 expression system that show potential of VP6 as a vaccine candidate against porcine  
107 rotavirus in future.

108

## 109 **Materials and Methods**

### 110 **Insect Cells and Silkworm Larvae**

111 Initially, Bm5 cells were maintained at 27°C in Sf-900II medium (Thermo Fisher  
112 Scientific K. K., Tokyo, Japan) supplemented with 1% antimycotic-antibiotic solution  
113 (Thermo Fisher Scientific K. K.) and 10% fetal bovine serum (Sigma Aldrich Japan,  
114 Tokyo, Japan). The fifth instar silkworm larvae were purchased from Ehimesansyu  
115 (Ehime, Japan), and reared on an artificial diet, Silkmate S2 (Nosan, Yokohama, Japan).

116

## 117 **Construction of Recombinant Plasmids and Baculoviruses**

118 First, the *VP6* gene of the porcine rotavirus A (KS14 strain) was amplified by PCR for  
119 its subsequent expression of VP6 (Table 1). Primer sets Rota-VP6-F and Rota-VP6-R  
120 were used in PCR. Next, the amplified gene was inserted into pFastbac:L21>30k6G ( $\pm$ )-  
121 Flag-Strep-tag II-TEV-Spytag002-StuI, downstream of the Spytag002 sequence [25].  
122 Each resulting plasmid was then transformed into *E. coli* BmDH10Bac to construct a  
123 recombinant *B. mori* nucleopolyhedrovirus (BmNPV) containing the VP6 gene [26].  
124 VP6 was then attached with the signal peptide of 30k6G protein that encodes a 30 kDa  
125 lipoprotein in silkworms [27], to obtain 30k-T-VP6 (Fig. 1). 30k-T-VP6 was expressed  
126 in silkworm larvae using recombinant BmNPV.

127 VP6 was also expressed without a signal sequence at its N-terminus (T-VP6, Fig. 1)  
128 and was similar to the native form of VP6. PCR was performed using the primer set,  
129 Rota-VP6-F2 and Rota-VP6-R2 (Table 1). The *VP6* gene thus obtained from PCR did  
130 not have sequence encoding the signal peptide of the silkworm. The amplified DNA  
131 after phosphorylation were allowed to self-ligate. Each resulting plasmid was  
132 transformed into *E. coli* BmDH10Bac cell to construct a recombinant BmNPV.

133 The *VP7* gene of rotavirus A (KS14 strain) was also used to construct recombinant  
134 BmNPV for VP7 by following the above protocol. First, the primer set Rota-VP7-F and  
135 Rota-VP7-R (Table 1) was used to amplify the *VP7* gene, and the amplified gene was  
136 inserted into pFastbac:L21>30k6G( $\pm$ )-Flag-Strep-tag II-TEV-Spytag002-StuI at the  
137 downstream of the Spytag002 sequence. VP7 was also attached to the signal peptide of  
138 30k6G protein to obtain 30k-T- $\Delta$ VP7. Now, the *VP7* gene encoding its soluble domain  
139 (30k-T- $\Delta$ VP7, Fig. 1) was inserted into the vector to express VP7 in its soluble form.

140 Finally, the constructed plasmids were transformed into *E. coli* BmDH10Bac cells to  
141 produce recombinant BmNPV.

142 Additionally, the *VP7* gene containing the PA-tag sequence encoding VP7-PA (Fig.  
143 1) was amplified via PCR using a primer set, Rota-VP7-F2 and Rota-VP7-PA-R (Table  
144 1) to express full-length VP7. The amplified gene was inserted into pFastbac1 (Thermo  
145 Fisher Scientific K. K.), and the resulting plasmid was transformed into *E. coli*  
146 BmDH10Bac to construct recombinant BmNPV.

147 The extracted recombinant BmNPVs were transfected into Bm5 cells to prepare  
148 recombinant BmNPV using FuGENE HD Transfection Reagent (Promega, Madison,  
149 WI, USA), according to the manufacturer's protocol. P3 viral solution was used to  
150 infect Bm5 cells and silkworm larvae.

151

### 152 **Expression of Each Protein in Insect Cells and Silkworm Larvae**

153 First, recombinant baculovirus solutions were used to infect Bm5 cells in 6-well plates  
154 and were injected into silkworm larvae. Next, the suspension of insect cells was  
155 centrifuged at  $20,000 \times g$  to isolate the culture supernatant from cell cultures. Further,  
156 the cell pellets were suspended in the same volume of phosphate-buffered saline (PBS,  
157 pH 7.4) as the culture supernatant and then sonicated to disrupt the cells. Finally,  
158 centrifugation was performed at  $20,000 \times g$  to separate the soluble from the insoluble  
159 fraction.

160

### 161 **Purification of Each Protein Using Affinity Gels**

162 T-VP6, 30k-T-VP6, and 30k-T- $\Delta$ VP7 were purified from silkworm hemolymph or the  
163 supernatant of the fat body homogenate using Strep-Tactin Sepharose (IBA GmbH,

164 Göttingen, Germany). First, the hemolymph was diluted 10-fold with ST buffer (100  
165 mM Tris-HCl, 150 mM NaCl, and 1 mM EDTA, pH 8.0) and loaded onto a Strep-Tactin  
166 Sepharose column equilibrated with PBS. Next, the resin was washed with a 20-bed  
167 volume of ST buffer, and the proteins were eluted NaOH (0.1 N). The eluent was then  
168 quickly neutralized with 2 M glycine-HCl buffer when NaOH was used. The fat body  
169 was first suspended in ST buffer and disrupted via sonication during T-VP6 purification.  
170 The homogenate was then centrifuged at  $10,000 \times g$  to obtain the soluble fraction for  
171 further protein purification.

172 VP7-PA was purified from silkworm hemolymph using Anti PA-tag antibody beads  
173 (FUJIFILM Wako Chemicals, Osaka, Japan), according to the previous paper [28].  
174 First, the hemolymph was diluted 10-fold with TBS buffer (20 mM Tris-HCl, 150 mM  
175 NaCl, pH 7.5), loaded onto Anti PA-tag antibody beads, and equilibrated with ST buffer.  
176 Next, a 20-bed volume of TBS was used to wash the resin, and the target proteins were  
177 separated using 0.1 M glycine-HCl buffer (pH 3.0). The eluent was quickly neutralized  
178 with 1M Tris-HCl buffer (pH 9.0). Finally, the Pierce BCA Protein Assay kit (Thermo  
179 Fisher Scientific K.K.) was used to measure protein concentration following the  
180 manufacturer's instructions.

181 Each recombinant protein was purified from dozens of silkworm larvae several  
182 times and confirmed these properties.

183

#### 184 **Deglycosylation of Purified Protein**

185 Briefly, glycopeptidase F (PNGase F; Takara Bio, Otsu, Japan) was used to remove *N*-  
186 glycans from the purified protein. The purified proteins were treated with PNGase F

187 under denaturing conditions, following the manufacturer's instructions. Finally, western  
188 blotting was performed to analyze the purified proteins after the treatment.

189

### 190 **Centrifugation of Purified VP7-PA and 30k-T-ΔVP7**

191 First, purified VP7 (2 mL) was centrifuged at  $122,000 \times g$  for 1 h on a 20% sucrose  
192 cushion (0.8 mL). Then, 1 mL (total 2 mL) of the sample fraction was collected,  
193 followed by collection of a 20% sucrose fraction (0.8 mL). The pellets were then  
194 suspended in 100  $\mu$ L of PBS. Finally, the proteins in each fraction were analyzed by  
195 sodium dodecyl sulfate polyacrylamide gel electrophoresis (SDS-PAGE).

196

### 197 **SDS-PAGE and Western Blot**

198 Briefly, SDS-PAGE was performed using 10% or 12% polyacrylamide gels. The  
199 proteins were first stained with Coomassie Brilliant Blue. They were then transferred  
200 from a gel onto a polyvinylidene fluoride membrane using the Mini Trans-Blot  
201 Electrophoretic Transfer Cell (Bio-Rad, Hercules, CA, USA) for western blot. Next, the  
202 membrane was incubated with 10,000-fold diluted anti-strep-Tag II (MEDICAL &  
203 BIOLOGICAL LABORATORIES, Nagoya, Japan) in TBS-T at room temperature for 1  
204 h after blocking with 5% skim milk in TBS-Tween 20 (TBS-T, pH 7.6). A 10,000-fold  
205 diluted goat anti-rabbit IgG horseradish peroxidase (HRP)-linked secondary antibody  
206 (Medical & Biological Laboratories) was then used. Finally, specific proteins were  
207 detected using Immobilon Western Chemiluminescent HRP Substrate (Merck Millipore,  
208 Billerica, MA, USA) and a Fluor-S Max Multi-Imager (Bio-Rad).

209

### 210 **Transmission Electron Microscopy**

211 Briefly, the samples were placed onto a grid with a support film (Nisshin EM, Tokyo,  
212 Japan) and negatively stained with 2.5% phosphotungstic acid. Further, transmission  
213 electron microscopy (TEM) was performed using a transmission electron microscope  
214 (JEM-2100F, JEOL, Ltd., Tokyo, Japan) operated at 100 kV.

215

## 216 **Results**

### 217 **Expression of VP6 and VP7 in Silkworm Larvae**

218 Rotavirus structural protein, VP6, has been previously purified from the culture  
219 supernatant and lysed insect cells and plants [12, 13, 15, 29]. In our study, we used a 30  
220 kDa lipoprotein signal peptide, 30k6G, obtained from silkworm. VP6 attached to the  
221 signal peptide and linked with FLAG-tag and strep-tag II (30k-T-VP6) was expressed to  
222 facilitate the purification of recombinant VP6 protein in silkworm larvae. This signal  
223 peptide permits the efficient secretion of expressed proteins into the hemolymph of  
224 silkworm larvae [24]. Similarly, VP7 attached to the signal peptide and linked to FLAG-  
225 tag and strep-tag II, was expressed with 30k-T- $\Delta$ VP7 (Fig. 1). The two hydrophobic  
226 domains of VP7 at the N-terminus were removed for efficient secretion into the  
227 hemolymph. Additionally, full-length VP7 linked with the PA-tag at its C-terminus was  
228 expressed.

229 Fig. 2a illustrates the successful expression of T-VP6 and 30k-T-VP6 in silkworm  
230 larvae. T-VP6 was detected in the soluble and insoluble fractions of the infected fat  
231 body tissue, but not in the hemolymph. Conversely, 30k-T-VP6 was observed in the fat  
232 body fractions as well as in hemolymph. These results show that the 30k6G signal  
233 peptide aided the efficient expression of VP6 in the silkworm hemolymph. Also, VP7-  
234 PA and 30k-T- $\Delta$ VP7 were expressed in both fat body and hemolymph fractions of

235 silkworm larvae (Fig. 2b). Interestingly, despite VP7-PA possessing two hydrophobic  
236 domains at its N-terminus, it was correctly secreted into the hemolymph [30].

237

### 238 **Purification of VP6 and VP7 from Silkworm Larvae**

239 Affinity chromatography was used to purify T-VP6 and 30k-T-VP6 from the soluble  
240 fractions of the fat body homogenate and hemolymph, respectively (Fig. 3a). The  
241 molecular weight of 30k-T-VP6 was slightly higher than that of T-VP6; however, it was  
242 seen as a band at approximately 45 kDa on SDS-PAGE. It was observed that the  
243 expressed 30k-T-VP6 migrated to the secretory pathway of the host cells and was then  
244 secreted into the hemolymph due to the presence of the 30k6G signaling peptide in  
245 VP6. After PNGase F treatment, the molecular weight of 30k-T-VP6 was reduced, as  
246 detected by a shift in band position on SDS-PAGE, whereas that of T-VP6 was  
247 unchanged (Fig. 3b). These results indicate that *N*-glycosylation contributes to higher  
248 molecular weight of the 30k-T-VP6 product via glycosylation pathway in the silkworm.  
249 Moreover, VP6 is a major capsid protein of rotavirus and is known to form  
250 nanoparticles or nanotubes [12, 13]. Therefore, we investigated the morphology of  
251 purified VP6 fractions using TEM. Figure 3c shows that T-VP6 formed nanoparticles  
252 with greater diameters compared to nanoparticles formed by 30k-T-VP6. These results  
253 also indicate that *N*-glycosylation of 30k-T-VP6 inhibited the formation of the VLPs of  
254 VP6. Furthermore, the amounts of T-VP6 and 30k-T-VP6 obtained upon purification  
255 were 330 and 50  $\mu$ g protein per larva, respectively. Totally, 37 mg of T-VP6 and 1.9 mg  
256 of 30k-T-VP6 were purified from 112 and 37 silkworm larvae, respectively.

257 Further in our procedure, affinity chromatography was used to purify VP7-PA and  
258 30k-T- $\Delta$ VP7 from the hemolymph of silkworms. SDS PAGE analysis of VP7-PA and

259 30k-T-ΔVP7 show bands of purified protein at approximately 40 kDa (Fig. 4a). After  
260 PNGase F treatment, deglycosylated bands of each purified VP7 were detected at a  
261 position corresponding to lower molecular weight (Fig. 4b). This result indicates that  
262 both VP7-PA and 30k-T-ΔVP7 were *N*-glycosylated within the silkworm expression  
263 system. VP7 is an outer layer protein of rotaviruses, localized in the endoplasmic  
264 reticulum (ER) [31, 32]. This study showed that full-length native VP7, VP7-PA, and  
265 30k-T-ΔVP7 were secreted into the hemolymph in silkworm larvae through the  
266 secretory pathway. The purified VP7 proteins were centrifuged in a 20% sucrose  
267 cushion to investigate VP7 variants (Fig. 5a). Remarkably, VP7-PA was observed in the  
268 20% sucrose fraction, whereas 30k-T-ΔVP7 was not seen. This result indicates that  
269 VP7-PA is morphologically different from 30k-T-ΔVP7. However, nanoparticles were  
270 not observed in either sample when examined by TEM (Fig. 5b). Corresponding to the  
271 previous studies, the results of our study show that unlike VP6, VP7 does not form  
272 ordered structures in the absence of Ca<sup>2+</sup> ions [33]. Furthermore, the amounts of the  
273 purified VP7-PA and 30k-T-ΔVP7 reached 26 and 49 μg per larva, respectively. Totally,  
274 0.40 mg of VP7-PA and 27 mg of 30k-T-ΔVP7 were purified from 15 and 545 silkworm  
275 larvae, respectively.

276

## 277 **Discussion**

278 In this study, T-VP6 and 30k-T-VP6 were successfully purified from the fat body and  
279 hemolymph of silkworm larvae, respectively (Fig. 3a). The deglycosylation assay  
280 confirmed that 30k-T-VP6 obtained from the silkworm expression system was *N*-  
281 glycosylated (Fig. 3b). In addition, T-VP6 formed nanoparticles with greater diameters  
282 compared with nanoparticles formed by 30k-T-VP6 (Fig. 3c). Therefore, these results

283 suggest that introducing *N*-glycosylation of VP6 via the silkworm glycosylation  
284 pathway impedes the formation of VP6-derived VLPs. Previous reports indicate that  
285 when the VP1 of mouse polyomavirus is expressed with aberrant *N*-glycosylation in  
286 insect cells, VP1 remains in a monomeric form and only little formation of VLPs takes  
287 place [34]. It has also been reported earlier that although, adeno-associated virus type 2  
288 has three putative *N*-glycosylation sites, its capsid protein remains unglycosylated [35].  
289 These results show that *N*-glycosylation of viral capsid proteins is undesirable for the  
290 formation of viral particles in a virus-dependent manner. As a subunit vaccine, co-  
291 administration of the subunit vaccine with some adjuvants are needed for the induction  
292 of immune system in vivo to prevent the infectious-viral infection. Whereas, in the case  
293 of virus-like particles, the co-administration with any adjuvant is not required because  
294 virus-like particles have almost the same morphology of viruses and can solely induce  
295 the host's immune system. In this study, T-VP6 form nanoparticles with diameter of  
296 several dozens of nanometers such as a virus-like particle. T-VP6 is promising as a  
297 virus-like particle vaccine to porcine rotavirus.

298 This study further demonstrated that T-VP6 and 30k-T-VP6 were purified at 330 and  
299 50 µg protein per larva, respectively. However, the production of VP7-PA and 30k-T-  
300 ΔVP7 resulted in a lower amount of 26 µg and 49 µg protein per larva, respectively. In  
301 previous reports, the amount of simian rotavirus SA11 VP6 protein quantified using  
302 enzyme-linked immunoassay after purification was found to be as high as 58 µg/mL in  
303 the culture supernatant of insect cells [12]. According to some previous reports,  
304 amounts as high as 400 µg/larva were obtained in *Spodoptera frugiperda*, when VP2/6  
305 particles were purified by CsCl<sub>2</sub> density gradient centrifugation [36]. Here double and  
306 triple-layered VLPs were seen [36]. Conversely, the amounts of VP2/6/7 particles was

307 12.7 µg/larva after purification using CsCl<sub>2</sub> density gradient centrifugation in silkworm  
308 larvae [25]. The amounts of T-VP6 and 30k-T-VP6 obtained in this study were similar  
309 to those in previous reports. Therefore, obtaining more purified proteins is possible by  
310 scaling up the number of infected silkworms for potential applications in future vaccine  
311 development.

312 *VP7* gene has a sequence encoding two hydrophobic domains (H1 and H2) at the N-  
313 terminus of its product; however, the sequence encoding the first hydrophobic domain  
314 (H1) is not translated [31, 32]. H2 works as a signal peptide that is removed during  
315 entry into the ER. Notably, VP7 has no hydrophobic domains except H1 and H2.  
316 Therefore, theoretically, it should be secreted extracellularly after the removal of H2.  
317 However, VP7 is retained in the mammalian ER because of the Ile-9, Thr-10, and Gly-  
318 11 sequences at the N-terminus [32]. This study showed the expression of VP7s in the  
319 hemolymph as a secretory protein despite the presence of Ile-9, Thr-10, and Gly-11  
320 sequences in the VP7s (Fig. 2). Therefore, these results show that silkworm cells have  
321 diverse mechanisms for retaining mammalian cell proteins in the ER, warranting further  
322 investigation.

323 In this study, T-VP6, which forms nanoparticles, and 30k-T-VP6, which does not  
324 form nanoparticles, were purified from fat body and hemolymph in silkworm larvae,  
325 respectively. We have to dissect silkworm larvae and collect fat body when we purified  
326 nanoparticles based on VP6, whereas 30k-T-VP6 can be purified from hemolymph  
327 collected from silkworm larvae easily. Collection of fat body from silkworm larvae is  
328 more laborious than that of hemolymph. However, the amount of T-VP6 purified from  
329 fat body is higher than that of 30k-T-VP6 purified from hemolymph.

330

331 **Conclusion**

332 VP6 and VP7 of porcine rotavirus A KS14 were expressed in silkworm larvae and  
333 purified from fat body and hemolymph. Especially, 330 µg of T-VP6, which has with  
334 Strep-tag II and FLAG tag at its N-terminus, was purified from a larva and formed  
335 nanoparticles with diameter of several dozens of nanometers. *N*-glycosylation in VP6  
336 inhibited the formation of its nanoparticles. VP7-PA and 30k-T-ΔVP7, which have its  
337 native and 30k6G signal peptide at its N-terminus, respectively, were also purified from  
338 silkworm larvae and *N*-glycosylated. Sedimentation properties of two VP7s were  
339 slightly different. Totally, 37 mg of T-VP6 and 27 mg of 30k-T-ΔVP7 were purified  
340 from 112 and 545 silkworm larvae. silkworm larvae are promising host to produce  
341 subunit vaccines to porcine rotavirus.

342

343 **Acknowledgement** This work was supported by Research Institute of Green Science  
344 and Technology Fund for Research Project Support (2021-RIGST-21C02). in Shizuoka  
345 University.

346

347 **Compliance with Ethical Standards**

348 **Conflict of interest** All authors declare no conflict of interest related  
349 to this study.

350

351

352

353 **References**

354

355 [1] Folorunso, O. S. and Sebolai, O. M. (2020) Overview of the development, impacts,  
356 and challenges of live-attenuated oral rotavirus vaccines. *Vaccines (Basel)*. 8(3),  
357 341. <https://doi.org/10.3390/vaccines8030341>

358 [2] Bass, D. M., Mackow, E. R. and Greenberg, H. B. (1991) Identification and partial  
359 characterization of a rhesus rotavirus binding glycoprotein on murine enterocytes.  
360 *Virology*. 183(2), 602–610. [https://doi.org/10.1016/0042-6822\(91\)90989-o](https://doi.org/10.1016/0042-6822(91)90989-o)

361 [3] Crawford, S. E., Labbé, M., Cohen, J., Burroughs, M. H., Zhou, Y. J. and Estes, M.  
362 K. (1994) Characterization of virus-like particles produced by the expression of  
363 rotavirus capsid proteins in insect cells. *Journal of Virology*. 68(9), 5945–5952.  
364 <https://doi.org/10.1128/JVI.68.9.5945-5952.1994>

365 [4] Armah, G. E., Sow, S. O., Breiman, R. F., Dallas, M. J., Tapia, M. D., Feikin, D. R.,  
366 Binka, F. N., Steele, A. D., Laserson, K. F., Ansah, N. A., Levine, M. M., Lewis,  
367 K., Coia, M. L., Attah-Poku, M., Ojwando, J., Rivers, S. B., Victor, J. C.,  
368 Nyambane, G., Hodgson, A., Schödel, F., Ciarlet, M. and Neuzil, K. M. (2010)  
369 Efficacy of pentavalent rotavirus vaccine against severe rotavirus gastroenteritis in  
370 infants in developing countries in sub-Saharan Africa: a randomised, double-blind,  
371 placebo-controlled trial. *Lancet*. 376(9741), 606–614.  
372 [https://doi.org/10.1016/S0140-6736\(10\)60889-6](https://doi.org/10.1016/S0140-6736(10)60889-6)

373 [5] Zaman, K., Dang, D. A., Victor, J. C., Shin, S., Yunus, Md., Dallas, M. J., Podder,  
374 G., Vu, D. T., Le, T. P. M., Luby, S. P., Le, H. T., Coia, M. L., Lewis, K., Rivers, S.  
375 B., Sack, D. A., Schödel, F., Steele, A. D., Neuzil, K. M. and Ciarlet, M. (2010)  
376 Efficacy of pentavalent rotavirus vaccine against severe rotavirus gastroenteritis in

377 infants in developing countries in Asia: a randomised, double-blind, placebo-  
378 controlled trial. *Lancet*. 376(9741), 615–623. <https://doi.org/10.1016/S0140->  
379 [6736\(10\)60755-6](https://doi.org/10.1016/S0140-6736(10)60755-6)

380 [6] Kumar, P., Shukla, R. S., Patel, A., Pullagurla, S. R., Bird, C., Ogun, O., Kumru, O.  
381 S., Hamidi, A., Hoeksema, F., Yallop, C., Bines, J. E., Joshi, S. B. and Volkin, D. V.  
382 (2021) Formulation development of a live attenuated human rotavirus (RV3-BB)  
383 vaccine candidate for use in low- and middle-income countries. *Human Vaccines*  
384 and Immunotherapeutics. 17(7), 2298–2310.  
385 <https://doi.org/10.1080/21645515.2021.1885279>.

386 [7] Groome, M. J., Koen, A., Fix, A., Page, N., Jose, L., Madhi, S. A., McNeal, M.,  
387 Dally, L., Cho, I., Power, M., Flores, J. and Cryz, S. (2017) Safety and  
388 immunogenicity of a parenteral P2-VP8-P[8] subunit rotavirus vaccine in toddlers  
389 and infants in South Africa: a randomised, double-blind, placebo-controlled trial.  
390 *The Lancet Infectious Disease*. 17(8), 843–853. <https://doi.org/10.1016/S1473->  
391 [3099\(17\)30242-6](https://doi.org/10.1016/S1473-3099(17)30242-6).

392 [8] Groome, M. J., Fairlie, L., Morrison, J., Fix, A., Koen, A., Masenya, M., Jose, L.,  
393 Madhi, S. A., Page, N., McNeal, M., Dally, L., Cho, I., Power, M., Flores, J. and  
394 Cryz, S. (2020) Safety and immunogenicity of a parenteral trivalent P2-VP8  
395 subunit rotavirus vaccine: a multisite, randomised, double-blind, placebo-  
396 controlled trial. *The Lancet Infectious Diseases*. 20(7), 851–863.  
397 [https://doi.org/10.1016/S1473-3099\(20\)30001-3](https://doi.org/10.1016/S1473-3099(20)30001-3).

398 [9] Lakatos, K., McAdams, D., White, J. A. and Chen, D. (2020) Formulation and  
399 preclinical studies with a trivalent rotavirus P2-VP8 subunit vaccine. *Human*

400 Vaccines and Immunotherapeutics. 16(8), 1957–1968.  
401 <https://doi.org/10.1080/21645515.2019.1710412>.

402 [10] Afchangi, A., Jalilvand, S., Mohajel, N., Marashi, S. M. and Shoja, Z. (2019)  
403 Rotavirus VP6 as a potential vaccine candidate. Reviews in Medical Virology.  
404 29(2), e2027. <https://doi.org/10.1002/rmv.2027>

405 [11] Pêra, F. F., Mutepfa, D. L., Khan, A. M., Els, J. H., Mbewana, S., van Dijk, A. A.,  
406 Rybicki, E. P. and Hitzeroth, I. I. (2015) Engineering and expression of a human  
407 rotavirus candidate vaccine in *Nicotiana benthamiana*. Virology Journal. 12, 205.  
408 <https://doi.org/10.1186/s12985-015-0436-8>

409 [12] Plascencia-Villa, G., Mena, J. A., Castro-Acosta, R. M., Fabián, J. C., Ramírez, O.  
410 T. and Palomares, L. A. (2011) Strategies for the purification and characterization  
411 of protein scaffolds for the production of hybrid nanobiomaterials. Journal of  
412 Chromatography. B, Analytical Technologies in the Biomedical and Life Sciences.  
413 879(15–16), 1105–1111. <https://doi.org/10.1016/j.jchromb.2011.03.027>

414 [13] Lappalainen, S., Vesikari, T. and Blazevic, V. (2016) Simple and efficient  
415 ultrafiltration method for purification of rotavirus VP6 oligomeric proteins.  
416 Archives of Virology. 161(11), 3219–3223. [https://doi.org/10.1007/s00705-016-](https://doi.org/10.1007/s00705-016-2991-8)  
417 [2991-8](https://doi.org/10.1007/s00705-016-2991-8)

418 [14] Pastor, A. R., Rodríguez-Limas, W. A., Contreras, M. A., Esquivel, E., Esquivel-  
419 Guadarrama, F., Ramírez, O. T. and Palomares, L. A. (2014) The assembly  
420 conformation of rotavirus VP6 determines its protective efficacy against rotavirus  
421 challenge in mice. Vaccine. 32(24), 2874–2877.  
422 <https://doi.org/10.1016/j.vaccine.2014.02.018>

- 423 [15] Lappalainen, S., Tamminen, K., Vesikari, T. and Blazevic, V. (2013) Comparative  
424 immunogenicity in mice of rotavirus VP6 tubular structures and virus-like  
425 particles. *Human Vaccines and Immunotherapeutics*. 9(9), 1991–2001.  
426 <https://doi.org/10.4161/hv.25249>
- 427 [16] Malm, M., Tamminen, K., Lappalainen, S., Vesikari, T. and Blazevic, V. (2016)  
428 Rotavirus recombinant VP6 nanotubes act as an immunomodulator and delivery  
429 vehicle for Norovirus virus-like particles. *Journal of Immunology Research*. 2016,  
430 9171632. <https://doi.org/10.1155/2016/9171632>
- 431 [17] Zhou, B., Zhang, Y., Wang, X., Dong, J., Wang, B., Han, C., Yu, J. and Li, D.  
432 (2010) Oral administration of plant-based rotavirus VP6 induces antigen-specific  
433 IgAs, IgGs and passive protection in mice. *Vaccine*. 28(37), 6021–6027.  
434 <https://doi.org/10.1016/j.vaccine.2010.06.094>
- 435 [18] Yu, J. and Langridge, W. (2003) Expression of rotavirus capsid protein VP6 in  
436 transgenic potato and its oral immunogenicity in mice. *Transgenic Research*. 12(2),  
437 163–169. <https://doi.org/10.1023/a:1022912130286>
- 438 [19] Feng, H., Li, X., Song, W., Duan, M., Chen, H., Wang, T. and Dong, J. (2017) Oral  
439 administration of a seed-based bivalent rotavirus vaccine containing VP6 and  
440 NSP4 induces specific immune responses in mice. *Frontiers in Plant Science*. 8,  
441 910. <https://doi.org/10.3389/fpls.2017.00910>
- 442 [20] Rosales-Mendoza, S., Angulo, C. and Meza, B. (2016) Food-grade organisms as  
443 vaccine biofactories and oral delivery vehicles. *Trends in Biotechnology*. 34(2),  
444 124–136. <https://doi.org/10.1016/j.tibtech.2015.11.007>

- 445 [21] Minkner, R. and Park, E. Y. (2018) Purification of virus-like particles (VLPs)  
446 expressed in the silkworm *Bombyx mori*. *Biotechnology Letters*. 40(4), 659–666.  
447 <https://doi.org/10.1007/s10529-018-2516-5>
- 448 [22] Yao, L., Wang, S., Su, S., Yao, N., He, J., Peng, L. and Sun, J. (2012) Construction  
449 of a baculovirus-silkworm multigene expression system and its application on  
450 producing virus-like particles. *PLOS ONE*. 7(3), e32510.  
451 <https://doi.org/10.1371/journal.pone.0032510>
- 452 [23] Song, J. M. (2021) Parenteral, non-live rotavirus vaccine: recent history and future  
453 perspective. *Clinical and Experimental Vaccine Research*. 10(3), 203–210.  
454 <https://doi.org/10.7774/cevr.2021.10.3.203>
- 455 [24] Soejima, Y., Lee, J. M., Nagata, Y., Mon, H., Iiyama, K., Kitano, H., Matsuyama,  
456 M. and Kusakabe, T. (2013) Comparison of signal peptides for efficient protein  
457 secretion in the baculovirus-silkworm system. *Central European Journal of*  
458 *Biology*. 8, 1–7.
- 459 [25] Xu, J., Kato, T. and Park, E. Y. (2019) Development of SpyTag/SpyCatcher-bacmid  
460 expression vector system (SpyBEVS) for protein bioconjugations inside of  
461 silkworms. *International Journal of Molecular Sciences*. 20(17), 4228.  
462 <https://doi.org/10.3390/ijms20174228>
- 463 [26] Motohashi, T., Shimojima, T., Fukagawa, T., Maenaka, K. and Park, E. Y. (2005)  
464 Efficient large-scale protein production of larvae and pupae of silkworm by  
465 *Bombyx mori* nuclear polyhedrosis virus bacmid system. *Biochemical and*  
466 *Biophysical Research Communications*. 326(3), 564–569.  
467 <https://doi.org/10.1016/j.bbrc.2004.11.060>

- 468 [27] Ebihara, T., Xu, J., Tonooka, Y., Nagasato, T., Kakino, K., Masuda, A.,  
469 Minamihata, K., Kamiya, N., Nakatake, H., Chieda, Y., Mon, H., Fujii, T.,  
470 Kusakabe, T. and Lee, J. M. Active human and murine tumor necrosis factor  $\alpha$   
471 cytokines produced from silkworm baculovirus expression system. *Insects*. 12(6),  
472 517. <https://doi.org/10.3390/insects12060517>
- 473 [28] Fujii, Y., Kaneko, M., Neyazaki, M., Nogi, T., Kato, Y. and Takagi, J. (2014) PA  
474 tag: a versatile protein tagging system using a super high affinity antibody against  
475 a dodecapeptide derived from human podoplanin. *Protein Expression and*  
476 *Purification*. 95, 240–247. <https://doi.org/10.1016/j.pep.2014.01.009>
- 477 [29] Malm, M., Diessner, A., Tamminen, K., Liebscher, M., Vesikari, T. and Blazevic, V.  
478 (2019) Rotavirus VP6 as an adjuvant for bivalent Norovirus vaccine produced in  
479 *Nicotiana benthamiana*. *Pharmaceutics*. 11(5), 229.  
480 <https://doi.org/10.3390/pharmaceutics11050229>
- 481 [30] Kato, T., Kajikawa, M., Maenaka, K. and Park, E. Y. (2010) Silkworm expression  
482 system as a platform technology in life science. *Applied Microbiology and*  
483 *Biotechnology*. 85(3), 459–470. <https://doi.org/10.1007/s00253-009-2267-2>
- 484 [31] Stirzaker, S. C., Whitfeld, P. L., Christie, D. L., Bellamy, A. R. and Both, G. W.  
485 (1987) Processing of rotavirus glycoprotein VP7: implications for the retention of  
486 the protein in the endoplasmic reticulum. *The Journal of Cell Biology*. 105(6 Pt 2),  
487 2897–2903. <https://doi.org/10.1083/jcb.105.6.2897>
- 488 [32] Maass, D. R. and Atkinson, P. H. (1994) Retention by the endoplasmic reticulum of  
489 rotavirus VP7 is controlled by three adjacent amino-terminal residues. *Journal of*  
490 *Virology*. 68(1), 366–378. <https://doi.org/10.1128/JVI.68.1.366-378.1994>

- 491 [33] Dormitzer, P. R., Greenberg, H. B. and Harrison, S. C. (2000) Purified recombinant  
492 rotavirus VP7 forms soluble, calcium-dependent trimers. *Virology*. 277(2), 420–  
493 428. <https://doi.org/10.1006/viro.2000.0625>
- 494 [34] Ng, J., Koechlin, O., Ramalho, M., Raman, D. and Krauzewicz, N. (2007)  
495 Extracellular self-assembly of virus-like particles from secreted recombinant  
496 polyoma virus major coat protein. *Protein Engineering, Design and Selection*  
497 (PEDS). 20(12), 591–598. <https://doi.org/10.1093/protein/gzm062>
- 498 [35] Murray, S., Nilsson, C. L., Hare, J. T., Emmett, M. R., Korostelev, A., Ongley, H.,  
499 Marshall, A. G. and Chapman, M. S. (2006) Characterization of the capsid protein  
500 glycosylation of adeno-associated virus type 2 by high-resolution mass  
501 spectrometry. *Journal of Virology*. 80(12), 6171–6176.  
502 <https://doi.org/10.1128/JVI.02417-05>
- 503 [36] Molinari, P., Peralta, A. and Taboga, O. (2008) Production of rotavirus-like  
504 particles in *Spodoptera frugiperda* larvae. *Journal of Virological Methods*. 147(2),  
505 364–367. <https://doi.org/10.1016/j.jviromet.2007.09.002>
- 506

507

508

509

510 **Table 1** List of primers used in this study

Primer	5'-3'
Rota-VP6-F	ATGGAGGTTCTGTACTCATTGTC
Rota-VP6-R	CCCTCGAGTCACTTAACCAACATGCTTCTAATGG
Rota-VP6-F2	ATGGACTACAAGGACGACGACGAC
Rota-VP6-R2	GGTGGCGGTTTTTTTAGGAG
Rota-VP7-F	ATGTATGGTATTGAATATAACCACAGTTCT
Rota-VP7-R	CCCTCGAGGGGGTCACATCATACAATTCTAA
Rota-VP7-F2	CCCGGATCCATGTATGGTATTGAATATAACCAC
Rota-VP7-PA-R	CCCAAGCTTTTACACCACATCATCTTCGGCACCTGGCAT GGCAACGCCTGAACCACCACCTACTCTGTAATAAAAAG CTGCAG

511

512

513 **Figure legends**

514

515 **Fig. 1** Constructs of expressed VP6 and VP7. 30k6G shows the sequences encoding the  
516 signal peptide of 30k6G, a hemolymph protein of silkworm larvae. The tag sequence  
517 contains the sequences encoding Strep-Tag II and FLAG-tag

518

519 **Fig. 2** Expression of (a) VP6 and (b) VP7 in silkworm larvae. First, silkworm larvae  
520 were infected with recombinant BmNPV containing a recombinant protein expression  
521 cassette described in Materials and Methods section. Hemolymph and fat body were  
522 collected after 4–5 d. Next, the fat body was suspended in PBS and disrupted through  
523 sonication. After that, the homogenate was centrifuged, and the supernatant and the  
524 precipitate were collected individually. Hem, Sup, and Pre denote hemolymph,  
525 supernatant of fat body homogenate, and precipitate of fat body homogenate,  
526 respectively. Arrows indicate the expressed proteins

527

528 **Fig. 3** Purification of T-VP6 and 30k-T-VP6 from the fat body and hemolymph of  
529 silkworm larvae. (a) T-VP6 and 30k-T-VP6 were purified by Strep-Tactin Sepharose  
530 column chromatography as described in the Materials and Methods section. The  
531 purified proteins were analyzed using SDS-PAGE, and the gel was stained with  
532 Coomassie Brilliant Blue. Asterisks indicate the purified proteins. (b) Deglycosylation  
533 of T-VP6 and 30k-T-VP6 with PNGase F, using the procedure described in the Materials  
534 and methods section. (c) TEM images of purified T-VP6 and 30k-T-VP6. The black bars  
535 represent 100 nm

536

537 **Fig. 4** Purification of VP7-PA and 30k-T- $\Delta$ VP7 from the hemolymph of silkworm  
538 larvae. (a) VP7-PA and 30k-T- $\Delta$ VP7 were purified using Anti-PA-tag Antibody Beads  
539 and PA-Strep-Tactin Sepharose column chromatography, respectively, following the  
540 protocols described in Materials and Methods section. The purified proteins were  
541 analyzed using SDS-PAGE, and the gel was stained with Coomassie Brilliant Blue. The  
542 asterisks (\*) denote the purified proteins. (b) Deglycosylation of VP7-PA and 30k-T-  
543  $\Delta$ VP7 was performed with PNGase F treatment, as described in the Materials and  
544 Methods section

545

546 **Fig. 5** Properties of VP7-PA and 30k-T- $\Delta$ VP7. (a) Centrifugation of VP7-PA and 30k-T-  
547  $\Delta$ VP7 on 20% sucrose cushion was performed, as described in the Materials and  
548 Methods section. The fractionated proteins were analyzed using SDS-PAGE. (b) TEM  
549 images of purified VP7-PA and 30k-T- $\Delta$ VP7

Fig. 1 Kato et al.

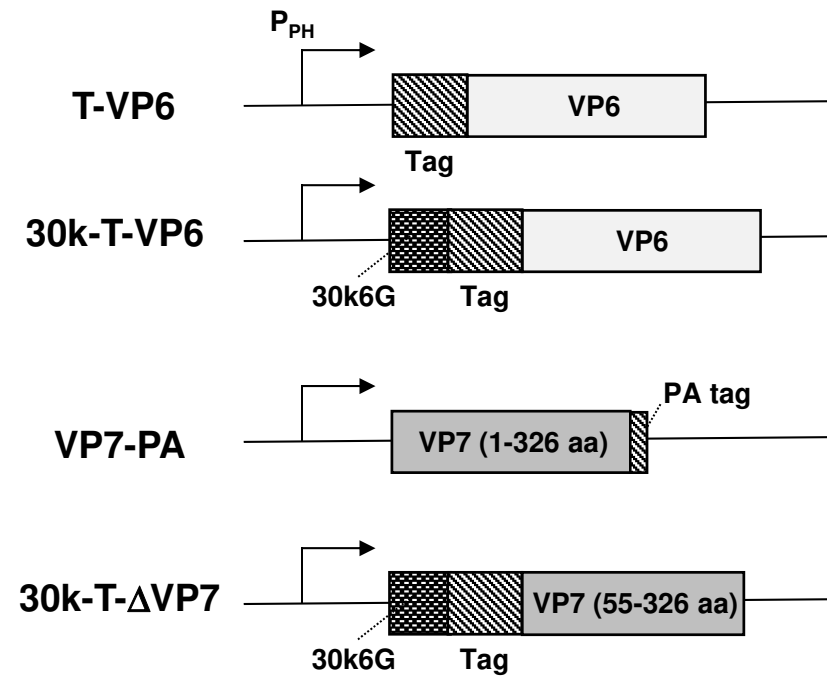


Fig. 2 Kato et al.

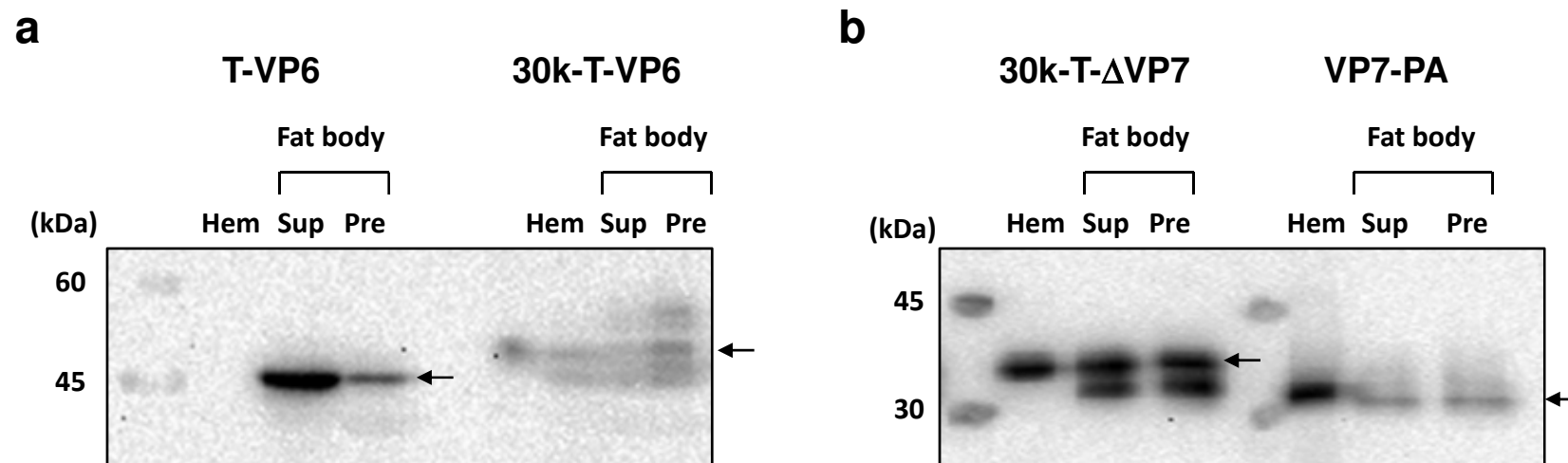


Fig. 3 Kato et al.

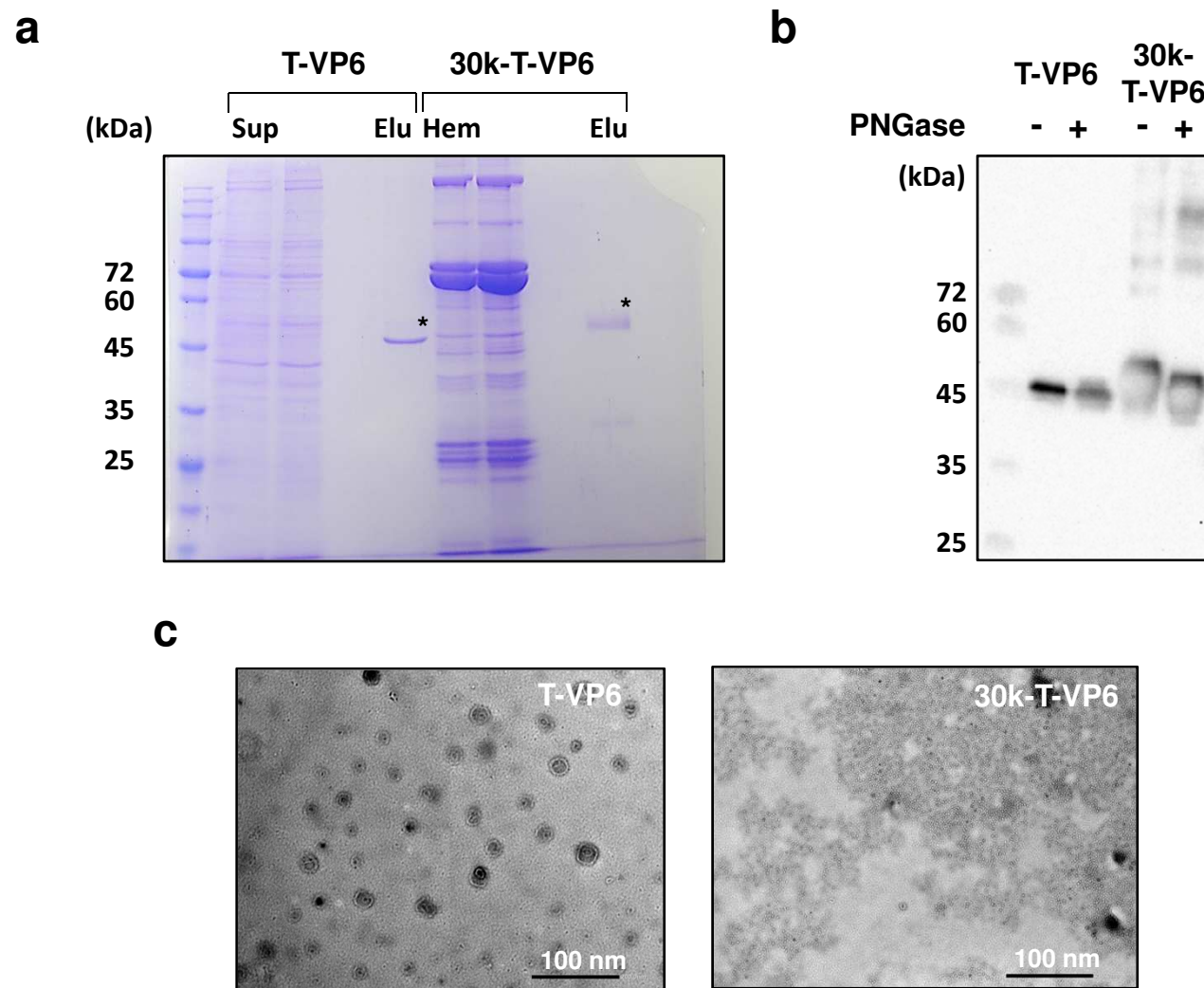
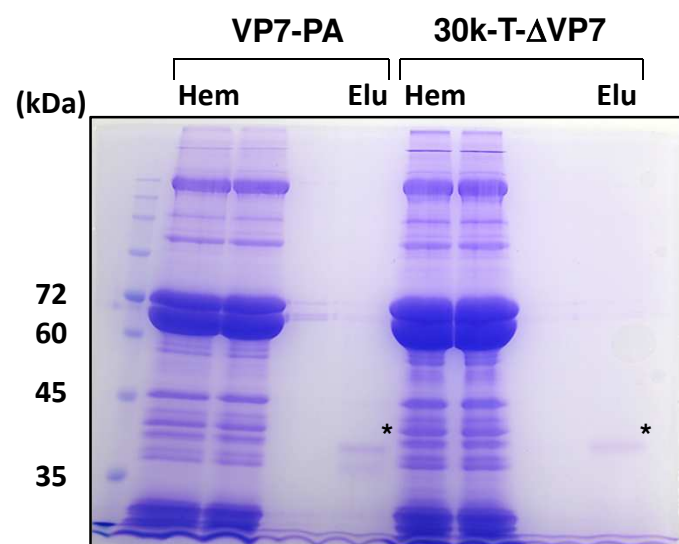


Fig. 4 Kato et al.

**a**



**b**

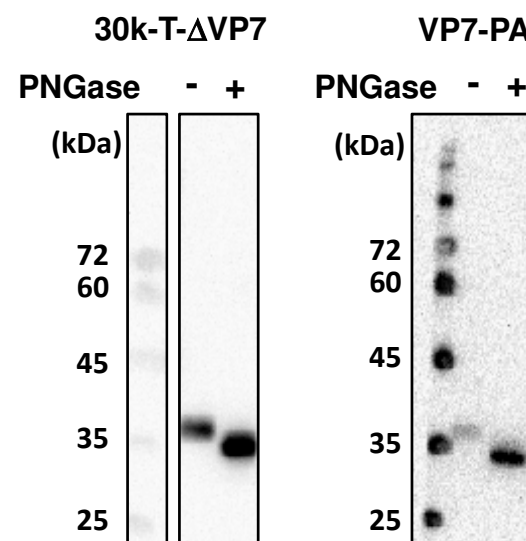
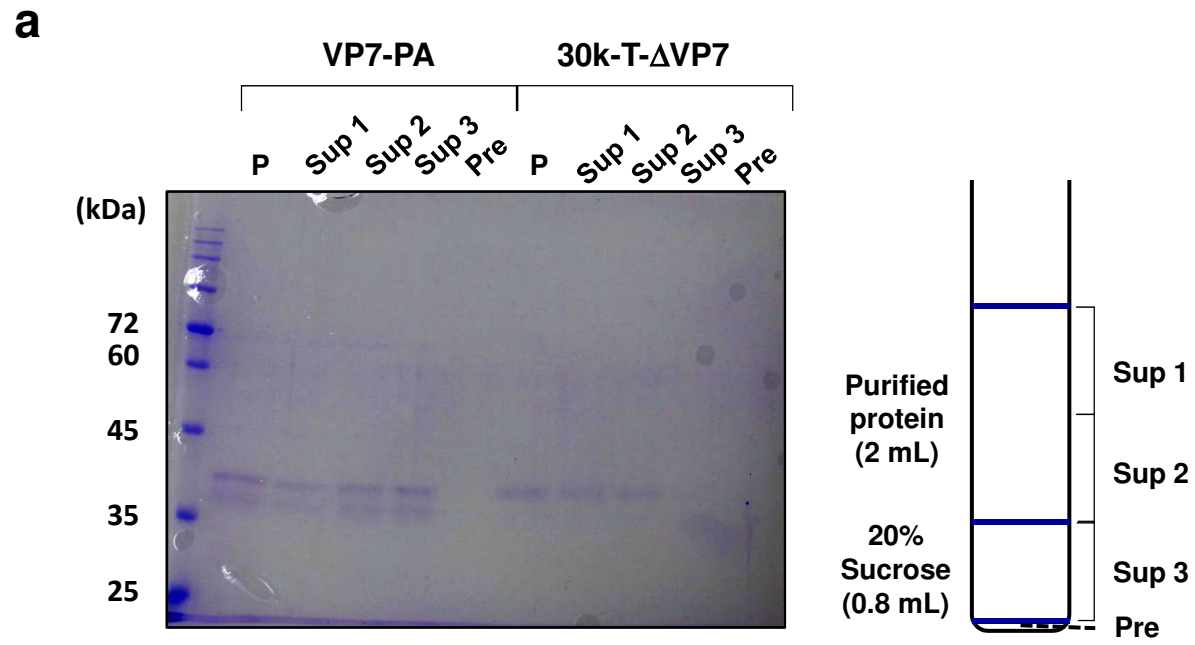


Fig. 5 Kato et al.



**b**

